Earth and Planetary Science Letters 528 (2019) 115827

Contents lists available at ScienceDirect

Earth and Planetary Science Letters

www.elsevier.com/locate/epsl

Recycling reduced iron at the base of magmatic orogens

Ming Tang [a,*], Cin-Ty A. Lee [a], Gelu Costin [a], Heidi E. Höfer [b]

[a] *Department of Earth, Environmental and Planetary Sciences, Rice University, Houston, TX 77005, USA*
[b] *Institut für Geowissenschaften, Johann Wolfgang Goethe-Universität, D-60054, Germany*

ARTICLE INFO

Article history:
Received 6 June 2019
Received in revised form 3 September 2019
Accepted 9 September 2019
Available online xxxx
Editor: F. Moynier

Keywords:
arclogite
magma redox
orogeny
garnet
magnetite
Fe valence

ABSTRACT

The Earth's continental crust is thought to originate from melting of the mantle, but it is too felsic and depleted in Fe relative to a primary mantle melt. This depletion in Fe is also commonly found in continental arc magmas and is often attributed to magnetite crystallization. However, Fe depletion in arc magmas coincides with an enrichment in ferric Fe relative to ferrous Fe, which cannot be explained by removal of a ferric Fe-rich mineral like magnetite. Deep-seated garnet pyroxenite arc cumulates (arclogites) have Fe-rich compositions that complement the Fe-depleted nature of the continental crust and continental arc magmas, and are likely candidates for the "missing link" between basaltic mantle magmas and the felsic continental crust. To test this suggestion, we present high precision in-situ Fe valence data for garnets in arclogites and reconstruct whole rock Fe valence states. We show that arclogites have low bulk $Fe^{3+}/\sum Fe$ due to the low $Fe^{3+}/\sum Fe$ of garnets and the lack of magnetite. At high pressures, garnet crystallizes, but magnetite does not, the former causing preferential accumulation of ferrous Fe at the base of magmatic orogens. Arclogite fractionation thus leads to the formation of oxidized felsic residual liquids ($Fe^{3+}/\sum Fe$ of 0.2-0.4). Such oxidation may profoundly influence the speciation of magmatic volatiles as well as the oxidative weathering capacity of the crust.

1. Introduction

The magmatic differentiation that leads to the formation of continental crust is characterized by Fe depletion, which is often referred to as "calc-alkaline" differentiation. This evolution to Fe depletion is seen in many arc magmas. In contrast, ocean basin magmatic series increase in Fe, a feature referred to as the "tholeiitic" differentiation series. What drives Fe depletion remains debated. A long-held view is that magnetite/spinel fractionation drives Fe depletion (Osborn, 1959; Sisson and Grove, 1993; Zimmer et al., 2010). However, owing to its high ferric iron content ($Fe^{3+}/\sum Fe$), magnetite fractionation should lead to more reduced magma compositions, which is inconsistent with the oxidized compositions of Fe-depleting magmatic series. Alternatively, Fe depletion can be driven by the fractionation of Fe-rich silicates, particularly garnet (Green and Ringwood, 1968; Tang et al., 2018). Indeed, the cumulates beneath magmatic orogens, where the crust is strongly Fe depleted, are mostly garnet-bearing pyroxenites (Chin et al., 2018; Ducea and Saleeby, 1998a; Ducea, 2002; Ducea and Saleeby, 1998b; Ducea et al., 2015; Erdman et al., 2016; Jagoutz and Schmidt, 2013; Lee et al., 2006; Tang et al., 2018; Tang et al., 2019), also known as arclogites (Lee and Anderson, 2015). In contrast to magnetite, magmatic garnet has been hypothesized to have low $Fe^{3+}/\sum Fe$, so its fractionation may act as a "redox filter" that drives simultaneous Fe depletion and magma oxidation (Tang et al., 2018).

Here, we first determine the $Fe^{3+}/\sum Fe$ of arclogite garnets to test the "redox filter" hypothesis. Then, we evaluate the effect of pressure on magnetite saturation in igneous differentiation. Most importantly, whatever fractionation process is responsible for Fe depletion must explain why Fe depletion is a feature of arc magmas traversing thick crust (continental arcs) and generally absent when the crust is thin (island arcs), as evidenced by the fact that the extent of Fe depletion in subduction zone magmas increases systematically with crustal thickness (Farner and Lee, 2017; Kuno, 1966; Tang et al., 2018).

2. Samples and methods

We examined arclogite samples from Arizona, USA. These arclogites are xenoliths from ∼25 Ma latites erupted through the Basin and Range-Colorado Plateau Transition Zone (BR-CP-TZ) in central Arizona, USA. U-Pb systematics of titanites suggest crystallization at 60 Ma or earlier (Erdman et al., 2016). The arclogites have been shown to represent deep crustal cumulates (45-80 km in depth) complementary in composition to

---

[*] Corresponding author.
E-mail address: tangmyes@gmail.com (M. Tang).

https://doi.org/10.1016/j.epsl.2019.115827

late Cretaceous-Paleogene Cordilleran plutonic rocks (Erdman et al., 2016). The arclogites are Fe-rich and are mostly composed of garnet and clinopyroxene with minor rutile, apatite and ilmenite. Some evolved (low Mg#; atomic Mg/(Mg+Fe)) cumulates also have appreciable amounts of amphibole.

Garnet is the main Fe-bearing silicate mineral in arclogites (modal abundance: 19-68%, average = 43%), thus its Fe valence state should control the bulk Fe oxidation state of silicate phases in arclogites. We determined garnet Fe^{3+}/$\sum$Fe in-situ by the electron microprobe flank method (Höfer, 2002; Höfer and Brey, 2007; Höfer et al., 1994, 2000; Li et al., 2018). All of the garnet crystals formed kelyphite rims during decompression (Fig. S2 in Supplementary File 3), making the bulk Fe^{3+}/$\sum$Fe analysis by Mössbauer spectroscopy unsuitable for whole rock Fe oxidation state reconstruction.

We carried out in-situ analyses of garnet Fe oxidation states on a JEOL JXA-8530F electron microprobe housed in the Earth Environmental and Planetary Sciences Department at Rice University. Briefly, the wavelengths and intensities of the soft Fe*L*a and Fe*L*b emission lines change with Fe valence in the sample. To determine the Fe *L*a and Fe *L*b measuring positions, the Fe *L*a and Fe *L*b spectra of almandine and andradite were collected at 15 kV accelerating voltage, 120 nA beam current with 50 s counting time per step and a step width of 0.03 mm. After normalizing the spectrum intensities to the Fe content, the positions for the Fe *L*a and Fe *L*b measurements were obtained at the maximum and minimum of the almandine-andradite difference spectrum, respectively. Before each session (24 h), the above “peak search” routine for Fe*K*a9 on Fe metal (integral mode, 25 kV, 80 nA) was done in order to recalibrate the spectrometer.

For the flank method measurements, we set the accelerating voltage to 15 kV and beam current to 120 nA. We also calibrated and introduced in the analysis recipe the routine elements present in garnets, so that the Fe *L*a and *L*b analysis was done during the full quantitative analysis. For elemental analysis we used the following mineral standards: almandine (Si, Al, Fe), jadeite (Na), orthoclase (K), plagioclase (Ca), rutile (Ti), olivine (Mg), rhodonite (Mn), chromite (Cr). Fe *L*a and Fe *L*b were added in the analysis recipe as two fake elements, where the “peak” positions of these fake elements were set to be the real Fe *L*a and Fe *L*b obtained from the almandine-andradite difference spectrum. The counting time for each *L*a and *L*b measurement was set at 300 s, with no background measurement. The last step was to measure each sample garnet 16 times (4 × 4 grid) using the exact same analytical protocol above, and determining the average Fe^{3+}/$\sum$Fe.

We measured nine garnet standards previously characterized for Fe^{3+}/$\sum$Fe by Mössbauer spectroscopy. The total Fe contents and Fe^{3+}/$\sum$Fe of these garnet standards are provided in Supplementary File 1. Among these garnet standards, we used Mir1, Mir2, AlmFRA1 and UA5 as calibration standards and UA10, UA17, Mir13, Mir23 and Damknolle as secondary standards. Fig. 1 compares our measured Fe^{3+}/$\sum$Fe and the Mössbauer results for the secondary garnet standards, together with our flank method results.

3. Results

The arclogite garnets are almandine-rich with high FeO$_T$ contents (15-25 wt.%, Supplementary File 2). The flank method measurements of garnet Fe^{3+}/$\sum$Fe agree within uncertainty with those determined from stoichiometry (Quinn et al., 2016) (Fig. 2a) and yield garnet Fe^{3+}/$\sum$Fe of 0.04–0.08. Such Fe^{3+}/$\sum$Fe values are significantly lower than those of basalts from the seafloor or in arcs (Kelley and Cottrell, 2009) (Fig. 2b). Garnet Fe^{3+}/$\sum$Fe also decreases systematically with whole-rock Mg# of the arclogites (Fig. 2b). This negative correlation between garnet Fe^{3+}/$\sum$Fe and whole-rock Mg# may appear to be inconsistent with a progressively increasing magma fO_2 with differentiation (Tang et al., 2018). However, Fe^{3+} partitioning in garnet is temperature dependent, making Fe^{3+} more compatible in garnets at high temperatures (Canil and O’Neill, 1996; Purwin et al., 2013; Wood et al., 2013). Because temperature and the Mg# of magma and cumulate both decrease with differentiation, we interpret the anticorrelation between garnet Fe^{3+}/$\sum$Fe and arclogite Mg# to largely reflect temperature control on Fe^{3+} uptake by arclogite garnets during their crystallization. Although subsolidus re-equilibration and recrystallization may blur the original igneous signatures, the Fe^{3+} signature of these arclogite garnets appears to have survived, possibly due to the sluggish diffusion of trivalent cations and the cold conditions these cumulates resided at (<700 °C; Erdman et al., 2016).

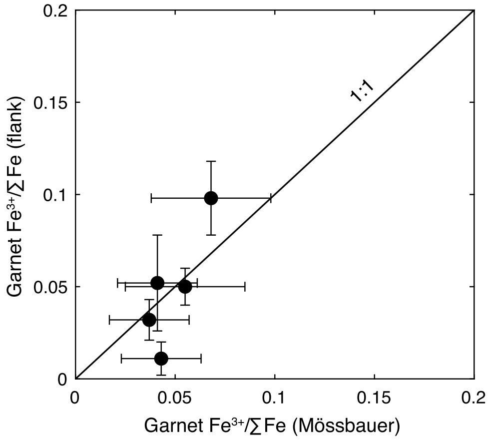

Fig. 1. Fe^{3+}/$\sum$Fe measured by electron microprobe flank method compared with the Mössbauer spectroscopy results for garnet standards Damknolle, UA10, UA17, Mir23 and Mir13. Except for Damknolle which is slightly lower, our electron microprobe flank method Fe^{3+}/$\sum$Fe data agree with the Mössbauer spectroscopy results within uncertainty. The flank method uncertainties are two standard errors (2 se) based on 16 measurements.

4. Discussion

The Fe^{3+}/$\sum$Fe of bulk arclogites is determined by Fe^{3+}/$\sum$Fe in silicate phases and the amount of Fe^{3+} rich oxides, i.e., magnetite. Below we first reconstruct the Fe^{3+}/$\sum$Fe of bulk silicates in arclogites. Then we evaluate the role of magnetite in magmatic differentiation.

4.1. Low Fe^{3+}/$\sum$ Fe in arclogite bulk silicates

The silicate phases in arclogites are dominated by garnet and clinopyroxene. The Fe^{3+}/$\sum$Fe of arclogite garnets are significantly lower than basaltic magmas from arcs and mid-ocean ridges (Fig. 2b). The Fe^{3+} contents in clinopyroxene can be estimated by the Fe^{3+} contents in garnets in the same samples using experimentally determined Fe^{3+} partitioning between garnet and clinopyroxene (Purwin et al., 2013). As temperature decreases from 1,300 to 800 °C, $(\text{Fe}^{3+}/\sum\text{Fe})_{cpx}/(\text{Fe}^{3+}/\sum\text{Fe})_{gt}$ increases from 1 to 2. We took the maximum $(\text{Fe}^{3+}/\sum\text{Fe})_{cpx}/(\text{Fe}^{3+}/\sum\text{Fe})_{gt}$ of 2 and calculated a maximum bound of Fe^{3+}/$\sum$Fe in clinopyroxene. The bulk silicate Fe^{3+}/$\sum$Fe was then calculated based on the Fe^{3+}/$\sum$Fe and FeO$_T$ contents in garnets and clinopyroxene and their proportions in arclogites. Except for the most primitive sample (Mg# = 0.77), whose FeO$_T$ content and Fe^{3+}/$\sum$Fe are close to MORB, all of the arclogites have high FeO$_T$ but low Fe^{3+}/$\sum$Fe relative to MORB (Fig. 3).

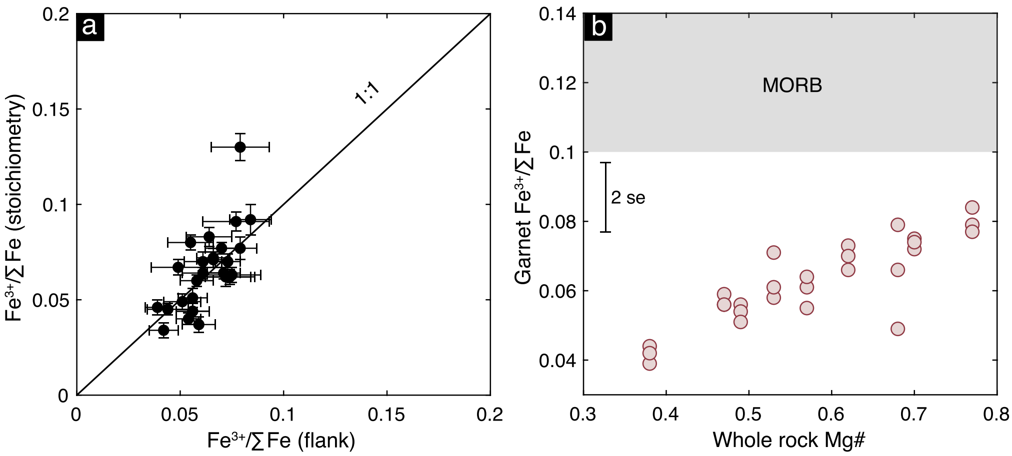

Fig. 2. (a) Comparison of $Fe^{3+}/\sum Fe$ determined by electron microprobe flank method vs. stoichiometry method for the arclogite garnets in this study. The uncertainties of both flank and stoichiometry method measurements are plotted as two standard errors (2 se) of 16 repeated measurements of each garnet crystal. The uncertainties of the stoichiometry method measurements may be well underestimated because they are very sensitive to the calibration schemes. (b) Measured garnet $Fe^{3+}/\sum Fe$ as a function of arclogite whole rock Mg#. We measured three garnets in each arclogite sample. The major element data for these arclogite samples are published at https://doi.org/10.1594/IEDA/111138. The MORB $Fe^{3+}/\sum Fe$ range (0.1-0.14), shown by the grey bar in (b), is from Bézos and Humler (2005), Berry et al. (2018) and Zhang et al. (2018). The $Fe^{3+}/\sum Fe$ of arc basalts ranges from MORB-like to more oxidized values and is highly debated (Brounce et al., 2014; Kelley and Cottrell, 2009; Lee et al., 2010; Mallmann and O'Neill, 2009). The data are provided in Supplementary File 2.

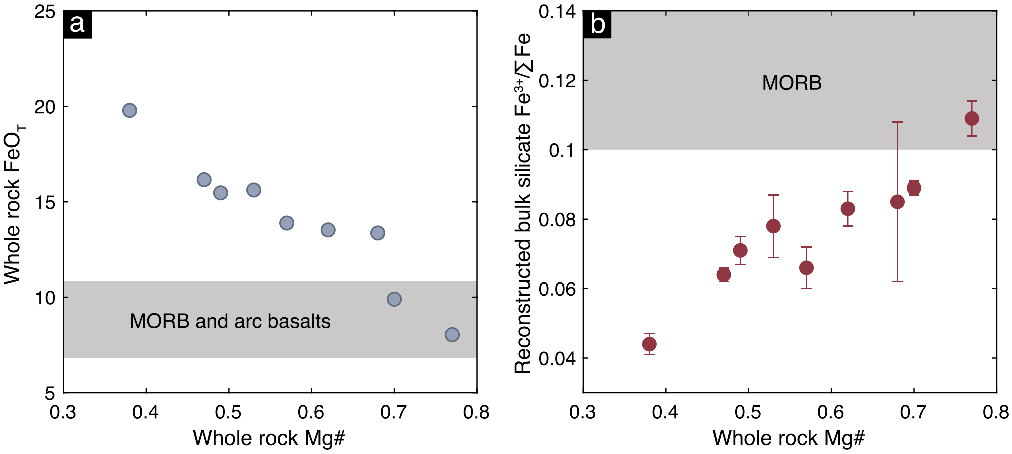

Fig. 3. (a) Arclogite whole rock FeO_T content vs. Mg#. The FeO_T contents of primitive MORB and arc basalts (MgO = 10 ± 1 wt.%), shown by the grey bar in (a), are from Keller et al. (2015) and our compilation, respectively. (b) Reconstructed $Fe^{3+}/\sum Fe$ of bulk silicates in arclogites. The $Fe^{3+}/\sum Fe$ of MORB is from the same sources as in Fig. 2. The error bars in (b) are two standard errors (2 se).

4.2. Magnetite saturation suppressed at high pressure

To evaluate the role of magnetite in the Fe-depleting magma series, we investigate here the effect of pressure on magnetite stability by carrying out alphaMELTS simulations ($n = 21{,}400$). We mapped the saturation fields of magnetite along the Fe-enriching (tholeiitic) and Fe-depleting (calc-alkaline) liquid lines of descent as represented by average mid-ocean ridge and Andean arc differentiation series, respectively (Supplementary File 3). We considered a range of oxygen fugacities from FMQ to FMQ+3 (denoted as $\log_{10}$ units of fO_2 relative to the fayalite-magnetite-quartz (FMQ) buffer). These thermodynamic simulations point to a strong effect of pressure on magnetite saturation. At pressures >1.2 GPa (~40 km), magnetite never saturates on the liquid line of descent of the Fe depleting series even when the oxygen fugacity is three log units above FMQ (Fig. 4b). The pressure effect on magnetite saturation is supported by the absence of magnetite in all arclogites, including those low Mg# ones which equilibrated with oxidized melts (>FMQ + 1, Tang et al., 2018). Further evidence for this pressure effect on magnetite saturation comes from the experiments by Matjuschkin et al. (2016), which show a dramatic reduction in the proportion of magnetite in the solid phases as experimental pressure increases from 0.5 to 1.5 GPa. At 1.5 GPa and 850–950 °C, magnetite is negligible (<0.1%) or completely absent even when the fO_2 is ~3 log units above FMQ (Matjuschkin et al., 2016). In fact, magnetite is also rare to absent in eclogites (Banno and Green, 1968).

The suppression of magnetite saturation at high pressure poses a major challenge to the magnetite-driven Fe depletion hypothesis in calc-alkaline differentiation series because Fe-depleted magmas are systematically more abundant in magmatic orogens where magmatic differentiation happens at great depths (Chiaradia, 2015; Ducea et al., 2015; Farner and Lee, 2017; Jagoutz, 2014; Profeta et al., 2015; Tang et al., 2018; Tang et al., 2019). Magnetite fractionation appears to occur largely at low pressures of differentiation associated with magmas traversing thin crust, such as at mid-ocean ridges and island arcs. At low pressures, magnetite is stable even at low fO_2 (FMQ), but its saturation occurs late (<3 wt.% MgO) in differentiation when Fe contents increase to levels high enough for saturation (Fig. 4a, c). Thus, there is an initial rise in magma FeO_T followed by a precipitous decline in FeO_T (Jenner et al., 2015; Tang et al., 2018).

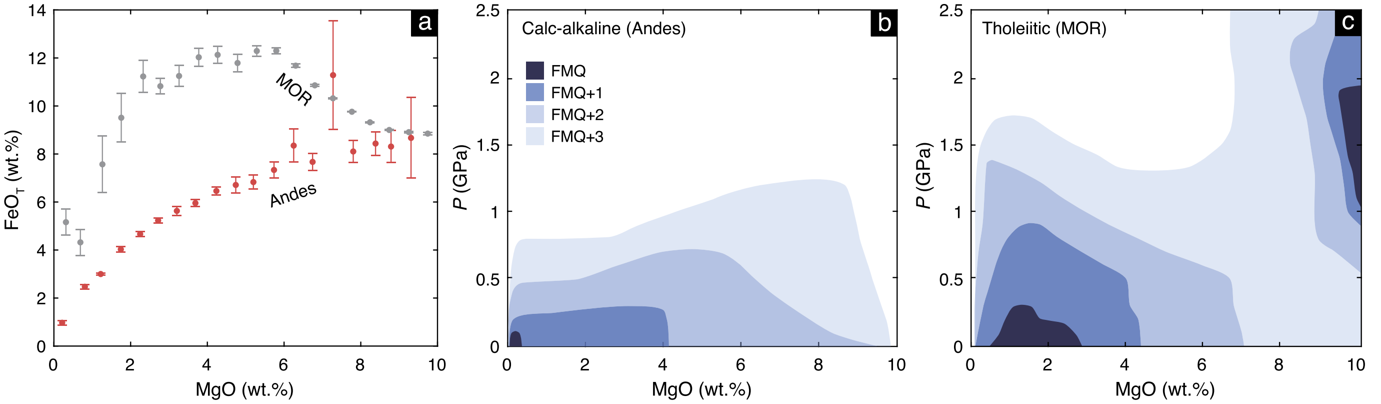

Fig. 4. Magnetite saturation fields for Fe-depleting (calc-alkaline) and Fe-enriching (tholeiitic) liquid lines of descent at different pressures. (a) Average calc-alkaline and tholeiitic differentiation trends were obtained using Andean (GeoRoc) and mid-ocean ridge igneous rocks (Keller et al., 2015), respectively. The error bars are two standard errors (2 se). These average differentiation trends between major/minor elements and MgO were fit by polynomial regressions, which we used to derive melt compositions for every 0.1 wt.% MgO increment. These incremental melt compositions were then used as inputs for alphaMELTS simulations (b & c). The alphaMELTS simulations were conducted under $P = 0$–2.5 GPa and $\Delta\text{FMQ}\log_{10} f\text{O}_2 = 0$–$3$. For the Fe-depleting series, we assumed 5 wt.% water in the system; for the Fe-enriching series, we assumed 0.2 wt.% water. Blue-shaded fields in (b) and (c) represent the stability fields of magnetite for different oxygen fugacities and melt compositions along the Fe-depleting (b) and Fe-enriching (c) differentiation series. See Supplementary File 3 for details. (For interpretation of the colors in the figure(s), the reader is referred to the web version of this article.)

In summary, the strong pressure effect on magnetite solubility leads to a seemingly counterintuitive conclusion that magnetite fractionation predominantly occurs in mid-ocean ridges and island arcs where magmas are mostly tholeiitic. In magmatic orogens such as the Andean continental arc, magnetite saturation is strongly suppressed, and Fe depletion is largely driven by garnet fractionation. These findings point to the fundamental role of crustal thickness in controlling magma redox evolution such that, with increasing crustal thickness, magmatic differentiation would lead to progressively more oxidized residual magmas as the effect of garnet increases.

5. Implications

The strongly Fe-depleted character of the continental crust mirrors that seen in Fe-depleted continental arcs, suggesting that magmatic orogenesis may be critical to making continents (Tang et al., 2018). The mass of recycled arclogites appears to be significant and is probably comparable to the mass of the remaining continental crust (Lee, 2014; Tang et al., 2019). Arclogite recycling should lead to coupled Fe depletion and $\text{Fe}^{3+}/\sum\text{Fe}$ increase of the remaining crust as long as the primary mantle or parental melts have $\text{Fe}^{3+}/\sum\text{Fe} > 0.1$ as appears to be the case. The $\text{Fe}^{3+}/\sum\text{Fe}$ of upper continental crust can be estimated using Fe^{3+}–Fe^{2+} mass balance. We arbitrarily divide the arclogites into high MgO (>13 wt.%) and low MgO (<13 wt.%) groups. For high MgO arclogites, the average reconstructed whole-rock FeO_T is 9.2 wt.% and the concentration-weighted mean $\text{Fe}^{3+}/\sum\text{Fe}$ is 0.094; for low MgO arclogites, the average reconstructed whole-rock FeO_T is 16.0 wt.% and the concentration-weighted mean $\text{Fe}^{3+}/\sum\text{Fe}$ is 0.066. We assume primary arc basalts to have 9 wt.% FeO_T and $\text{Fe}^{3+}/\sum\text{Fe}$ of 0.12 (~FMQ buffer). The initial $\text{Fe}^{3+}/\sum\text{Fe}$ of primary arc basalts is debated and could be higher (Brounce et al., 2014; Kelley and Cottrell, 2009), but the purpose of our calculation is to evaluate the relative change in magma redox conditions. We also assume limited magnetite fractionation through much of the Fe-depleting differentiation series in magmatic orogens. Figs. 5a and b show the FeO_T content and $\text{Fe}^{3+}/\sum\text{Fe}$ of the remaining crust as a function of the mass proportion of fractionated arclogite ($F_\text{arclogite}$). The $\text{Fe}^{3+}/\sum\text{Fe}$ of derivative melts increases exponentially with arclogite fractionation and Fe depletion (Fig. 5b, c), meaning that significant magma oxidation should only occur late (likely andesitic to dacitic) in differentiation. Magma $\text{Fe}^{3+}/\sum\text{Fe}$ should stay low in basaltic to andesitic differentiation due to the high initial FeO_T content of basalts. The relatively high $\text{Fe}^{3+}/\sum\text{Fe}$ of primitive arclogites (Fig. 3b) also suppresses early magma oxidation. This delayed magma oxidation allows for substantial sulfide precipitation in early differentiation as seen by continuous Cu depletion in continental arcs (Chiaradia, 2014; Lee et al., 2012).

Although the uncertainty in the proportions of high/low MgO arclogites in the fractionating assemblage results in uncertainty in melt FeO_T and $\text{Fe}^{3+}/\sum\text{Fe}$ for a given $F_\text{arclogite}$ (Fig. 5a, b), correlations between melt $\text{Fe}^{3+}/\sum\text{Fe}$ and FeO_T are less affected (Fig. 5c). Felsic magmas with ~5 wt.% FeO_T, which is equivalent to that of the average upper continental crust (Rudnick and Gao, 2014), should have a bulk $\text{Fe}^{3+}/\sum\text{Fe}$ of 0.2–0.4, consistent with various estimates (Lécuyer and Ricard, 1999). The rapid increase in melt $\text{Fe}^{3+}/\sum\text{Fe}$ at extremely low FeO_T could be unrealistic. In evolved magmas, amphibole may saturate and remove ferric Fe from the magma due to its near unity $\text{Fe}^{3+}/\text{Fe}^{2+}$ partitioning (King et al., 2000). In fact, amphibole is present in appreciable amounts in some of the low Mg# arclogites. Moreover, as felsic magmas rise into the shallow crust, magnetite may then saturate, limiting further oxidation (Fig. 4).

Crustal differentiation in magmatic orogens is no doubt formed through a complex combination of crystal fractionation, crustal remelting and melt/rock reaction. Our simplified model uses only the ferric/ferrous Fe mass balance and does not distinguish between crystal fractionation vs. crustal remelting. Deep crustal melting with eclogitic residues should generate similarly oxidized felsic melts.

A caveat in our redox budget calculation is that we only considered arclogite loss in continent formation. There is evidence that foundering eclogitic lower crust of gabbroic protoliths can also be important (Gao et al., 1998; Tang et al., 2015; Willbold and Stracke, 2010). We suggest that if the eclogitic lower crust undergoes partial melting before or during foundering, ferric Fe will rise with the magmas whereas ferrous Fe will sink with the garnets in the eclogitic residues, causing a net oxidation of the shallow crust in a way similar to arclogite fractionation.

After their formation, arclogites may eventually founder into the mantle and return ferrous Fe to the deep Earth (Fig. 6). This unique mass transfer across the Moho of magmatic orogens leads to a number of important implications. For example, the oxidized continental crust (Lécuyer and Ricard, 1999) may form from reduced mantle magmas without the need for massive interaction

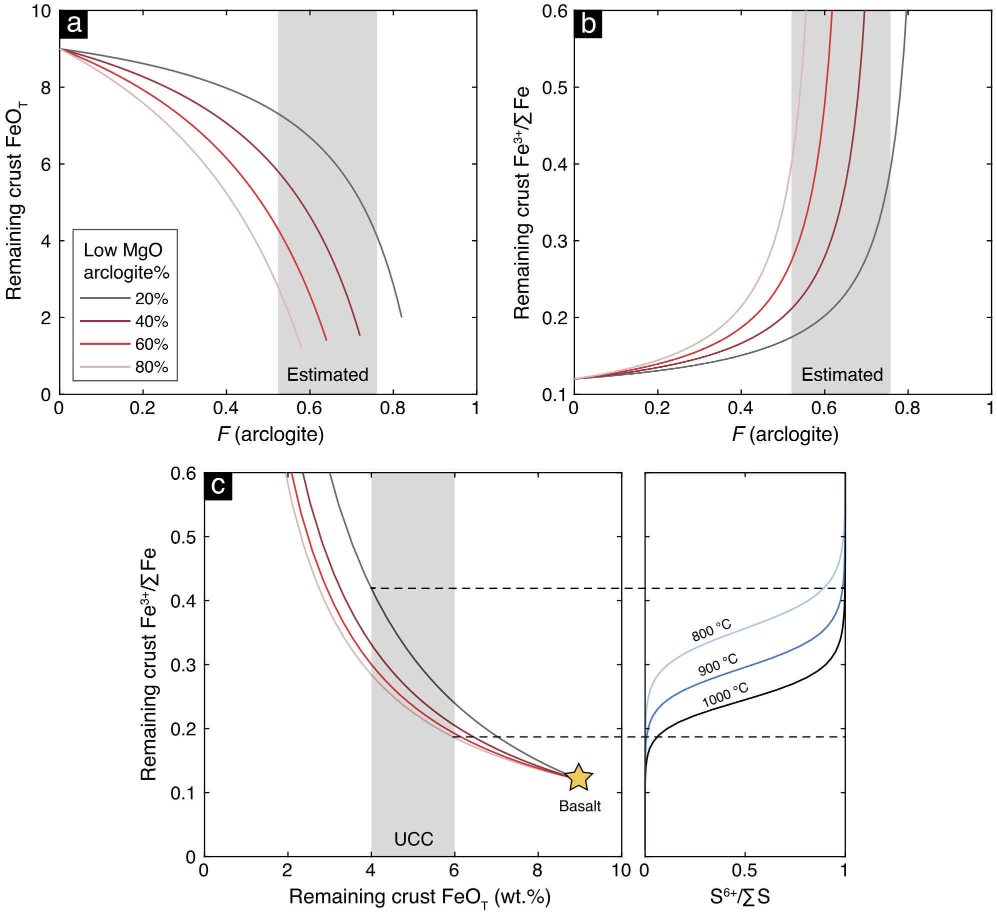

Fig. 5. Magma Fe depletion and oxidation as a consequence of arclogite fractionation. We considered a range of proportions of low/high MgO arclogite combinations denoted by the curve colors. The grey bars in (a) and (b) mark the estimated total mass proportions of arclogites with respect to primary arc basalts (Lee, 2014). Shown in (c) is the melt $Fe^{3+}/\sum Fe$ as a function of melt Fe depletion. The gray band in (c) denotes the average FeO_T content of the upper continental crust (UCC) from Rudnick and Gao (2014); the correlations between melt $S^{6+}/\sum S$ and $Fe^{3+}/\sum Fe$ at 800–1000 °C, typical of felsic magmas, are from Nash et al. (2019).

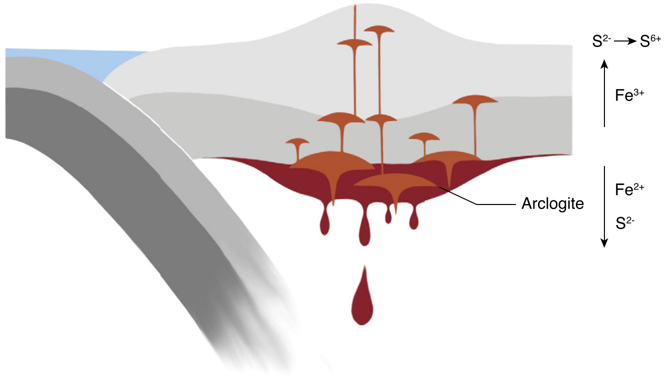

Fig. 6. Cartoon showing magma oxidation due to arclogite recycling at the base of magmatic orogens. Arclogite recycling removes reduced Fe (Fe^{2+}) from the magmas. Iron depletion also reduces sulfur solubility and drives sulfide crystallization. Magma $Fe^{3+}/\sum Fe$ will rise and eventually oxidize the remaining S in late stage differentiation.

with previously oxidized supracrustal materials. Although crustal assimilation is inevitable when magmas differentiate in the crust, we suggest the growth of oxidized continental crust may be largely driven by internal petrogenetic processes instead of interaction with the Earth's surface. In magmatic orogens, magma oxidation may eventually cause oxidation of sulfides to sulfate, e.g., S^{2-} to S^{6+} (Fig. 5c), releasing and mobilizing chalcophile elements like Cu during late stage differentiation in the upper crust. This may explain why most giant Cu porphyries are associated with Fe-depleted plutons and continental arcs (Cooke et al., 2005), but appear not to come from Cu-enriched parental magmas (Lee et al., 2012).

6. Conclusions

1. In-situ measurements show low $Fe^{3+}/\sum Fe$ (0.04-0.08) in garnets from arclogites, which represent the Fe-rich cumulates from magmatic orogens.
2. Magnetite saturation in magmatic differentiation is strongly dependent on pressure. At the base of magmatic orogens where the pressure is likely greater than 1 GPa, magnetite fractionation is probably negligible even when the magma is highly oxidized ((ΔFMQ $\log_{10} fO_2 \sim 3$).
3. Arclogites are Fe-rich but have bulk $Fe^{3+}/\sum Fe$ (<0.1) significantly lower than MORB and arc basalts due to low $Fe^{3+}/\sum Fe$ garnets and the absence of magnetite. Arclogite fractionation thus causes simultaneous Fe depletion and oxidation of the derivative evolved melts that form the shallow crust in magmatic orogens and probably most of the upper continental crust.

Acknowledgements

This work was supported by U.S. National Science Foundation grants to Lee (OCE-1338842, EAR-1347085, EAR-1850832). We thank Jianxin Gao for assistance in alphaMELTS simulation coding. Ming Tang is also grateful for the support from Chinese

Academy of Sciences (Z201706). We thank Simone Runyon and Claude Herzberg for their constructive reviews.

Appendix A. Supplementary material

Supplementary material related to this article can be found online at https://doi.org/10.1016/j.epsl.2019.115827.

References

Banno, S., Green, D.H., 1968. Experimental studies on eclogites: the roles of magnetite and acmite in eclogitic assemblages. Chem. Geol. 3, 21–32.

Berry, A.J., Stewart, G., O'Neill, H.St.C., Mallmann, G., Mallmann, J.F., 2018. A reassessment of the oxidation state of iron in MORB glasses. Earth Planet. Sci. Lett. 483, 114–123.

Bézos, A., Humler, E., 2005. The $Fe^{3+}/\sum Fe$ ratios of MORB glasses and their implications for mantle melting. Geochim. Cosmochim. Acta 69, 711–725.

Brounce, M., Kelley, K., Cottrell, E., 2014. Variations in $Fe^{3+}/\sum Fe$ of Mariana Arc Basalts and Mantle Wedge fO_2. J. Petrol. 55, 2513–2536.

Canil, D., O'Neill, H.S.C., 1996. Distribution of ferric iron in some upper-mantle assemblages. J. Petrol. 37, 609–635.

Chiaradia, M., 2014. Copper enrichment in arc magmas controlled by overriding plate thickness. Nat. Geosci. 7, 43.

Chiaradia, M., 2015. Crustal thickness control on Sr/Y signatures of recent arc magmas: an Earth scale perspective. Sci. Rep. 5.

Chin, E.J., Shimizu, K., Bybee, G.M., Erdman, M.E., 2018. On the development of the calc-alkaline and tholeiitic magma series: a deep crustal cumulate perspective. Earth Planet. Sci. Lett. 482, 277–287.

Cooke, D.R., Hollings, P., Walshe, J.L., 2005. Giant porphyry deposits: characteristics, distribution, and tectonic controls. Econ. Geol. 100, 801–818.

Ducea, M., Saleeby, J., 1998a. Crustal recycling beneath continental arcs: silica-rich glass inclusions in ultramafic xenoliths from the Sierra Nevada, California. Earth Planet. Sci. Lett. 156, 101–116.

Ducea, M.N., 2002. Constraints on the bulk composition and root foundering rates of continental arcs: a California arc perspective. J. Geophys. Res., Solid Earth 107. ECV 15-11–ECV 15-13.

Ducea, M.N., Saleeby, J.B., 1998b. The age and origin of a thick mafic–ultramafic keel from beneath the Sierra Nevada batholith. Contrib. Mineral. Petrol. 133, 169–185.

Ducea, M.N., Saleeby, J.B., Bergantz, G., 2015. The architecture, chemistry, and evolution of continental magmatic arcs. Annu. Rev. Earth Planet. Sci. 43, 299–331.

Erdman, M.E., Lee, C.-T.A., Levander, A., Jiang, H., 2016. Role of arc magmatism and lower crustal foundering in controlling elevation history of the Nevadaplano and Colorado Plateau: a case study of pyroxenitic lower crust from central Arizona, USA. Earth Planet. Sci. Lett. 439, 48–57.

Farner, M.J., Lee, C.-T.A., 2017. Effects of crustal thickness on magmatic differentiation in subduction zone volcanism: a global study. Earth Planet. Sci. Lett. 470, 96–107.

Gao, S., Zhang, B.-R., Jin, Z.-M., Kern, H., Ting-Chuan, L., Zhao, Z.-D., 1998. How mafic is the lower continental crust? Earth Planet. Sci. Lett. 161, 101–117.

Green, T.H., Ringwood, A.E., 1968. Genesis of the calc-alkaline igneous rock suite. Contrib. Mineral. Petrol. 18, 105–162.

Höfer, H.E., 2002. Quantification of Fe^{2+}/Fe^{3+} by electron microprobe analysis – new developments. Hyperfine Interact. 144, 239–248.

Höfer, H.E., Brey, G.P., 2007. The iron oxidation state of garnet by electron microprobe: its determination with the flank method combined with major-element analysis. Am. Mineral. 92, 873–885.

Höfer, H.E., Brey, G.P., Schulz-Dobrick, B., Oberhaensli, R., 1994. The determination of the oxidation state of iron by the electron microprobe. Eur. J. Mineral. 407 (418).

Höfer, H.E., Weinbruch, S., Mccammon, C.A., Brey, G.P., 2000. Comparison of two electron probe microanalysis techniques to determine ferric iron in synthetic wustite samples. Eur. J. Mineral. 12, 63–71.

Jagoutz, O., 2014. Arc crustal differentiation mechanisms. Earth Planet. Sci. Lett. 396, 267–277.

Jagoutz, O., Schmidt, M.W., 2013. The composition of the foundered complement to the continental crust and a re-evaluation of fluxes in arcs. Earth Planet. Sci. Lett. 371–372, 177–190.

Jenner, F.E., Hauri, E.H., Bullock, E.S., König, S., Arculus, R.J., Mavrogenes, J.A., Mikkelson, N., Goddard, C., 2015. The competing effects of sulfide saturation versus degassing on the behavior of the chalcophile elements during the differentiation of hydrous melts. Geochem. Geophys. Geosyst. 16, 1490–1507.

Keller, C.B., Schoene, B., Barboni, M., Samperton, K.M., Husson, J.M., 2015. Volcanic-plutonic parity and the differentiation of the continental crust. Nature 523, 301–307.

Kelley, K.A., Cottrell, E., 2009. Water and the oxidation state of subduction zone magmas. Science 325, 605–607.

King, P., Hervig, R., Holloway, J., Delaney, J., Dyar, M., 2000. Partitioning of Fe^{3+}/Fe_{total} between amphibole and basanitic melt as a function of oxygen fugacity. Earth Planet. Sci. Lett. 178, 97–112.

Kuno, H., 1966. Lateral variation of basalt magma type across continental margins and Island Arcs. Bull. Volcanol. 29, 195–222.

Lécuyer, C., Ricard, Y., 1999. Long-term fluxes and budget of ferric iron: implication for the redox states of the Earth's mantle and atmosphere. Earth Planet. Sci. Lett. 165, 197–211.

Lee, C.-T.A., Anderson, D.L., 2015. Continental crust formation at arcs, the arclogite "delamination" cycle, and one origin for fertile melting anomalies in the mantle. Sci. Bull. 60, 1141–1156.

Lee, C.-T.A., Luffi, P., Le Roux, V., Dasgupta, R., Albarede, F., Leeman, W.P., 2010. The redox state of arc mantle using Zn/Fe systematics. Nature 468, 681–685.

Lee, C.-T.A., Luffi, P., Chin, E.J., Bouchet, R., Dasgupta, R., Morton, D.M., Le Roux, V., Yin, Q.-z., Jin, D., 2012. Copper systematics in arc magmas and implications for crust-mantle differentiation. Science 336, 64–68.

Lee, C.T.A., 2014. 4.12 – Physics and chemistry of deep continental crust recycling. In: Holland, H.D., Turekian, K.K. (Eds.), Treatise on Geochemistry, second edition. Elsevier, Oxford, pp. 423–456.

Lee, C.T.A., Cheng, X., Horodyskyj, U., 2006. The development and refinement of continental arcs by primary basaltic magmatism, garnet pyroxenite accumulation, basaltic recharge and delamination: insights from the Sierra Nevada, California. Contrib. Mineral. Petrol. 151, 222–242.

Li, X., Song, S., Zhang, L., Höfer, E.H., 2018. Application of microprobe-based flank method analysis of Fe^{3+} in garnet of North Qilian eclogite and its geological implication. Sci. Bull. 63, 300–305.

Mallmann, G., O'Neill, H.S.C., 2009. The crystal/melt partitioning of V during mantle melting as a function of oxygen fugacity compared with some other elements (Al, P, Ca, Sc, Ti, Cr, Fe, Ga, Y, Zr and Nb). J. Petrol. 50, 1765–1794.

Matjuschkin, V., Blundy, J.D., Brooker, R.A., 2016. The effect of pressure on sulphur speciation in mid- to deep-crustal arc magmas and implications for the formation of porphyry copper deposits. Contrib. Mineral. Petrol. 171, 66.

Nash, W.M., Smythe, D.J., Wood, B.J., 2019. Compositional and temperature effects on sulfur speciation and solubility in silicate melts. Earth Planet. Sci. Lett. 507, 187–198.

Osborn, E.F., 1959. Role of oxygen pressure in the crystallization and differentiation of basaltic magma. Am. J. Sci. 257, 609–647.

Profeta, L., Ducea, M.N., Chapman, J.B., Paterson, S.R., Gonzales, S.M.H., Kirsch, M., Petrescu, L., DeCelles, P.G., 2015. Quantifying crustal thickness over time in magmatic arcs. Sci. Rep. 5.

Purwin, H., Lauterbach, S., Brey, G.P., Woodland, A.B., Kleebe, H.-J., 2013. An experimental study of the Fe oxidation states in garnet and clinopyroxene as a function of temperature in the system $CaO–FeO–Fe_2O_3–MgO–Al_2O_3–SiO_2$: implications for garnet–clinopyroxene geothermometry. Contrib. Mineral. Petrol. 165, 623–639.

Quinn, R.J., Valley, J.W., Zeb Page, F., Fournelle, J.H., 2016. Accurate determination of ferric iron in garnets. Am. Mineral. 101, 1704–1707.

Rudnick, R.L., Gao, S., 2014. 4.1 – Composition of the continental crust. In: Holland, H.D., Turekian, K.K. (Eds.), Treatise on Geochemistry, second edition. Elsevier, Oxford, pp. 1–51.

Sisson, T.W., Grove, T.L., 1993. Experimental investigations of the role of H_2O in calc-alkaline differentiation and subduction zone magmatism. Contrib. Mineral. Petrol. 113, 143–166.

Tang, M., Rudnick, R.L., McDonough, W.F., Gaschnig, R.M., Huang, Y., 2015. Europium anomalies constrain the mass of recycled lower continental crust. Geology 43, 703–706.

Tang, M., Erdman, M., Eldridge, G., Lee, C.-T.A., 2018. The redox "filter" beneath magmatic orogens and the formation of continental crust. Sci. Adv. 4.

Tang, M., Lee, C.-T.A., Chen, K., Erdman, M., Costin, G., Jiang, H., 2019. Nb/Ta systematics in arc magma differentiation and the role of arclogites in continent formation. Nat. Commun. 10, 235.

Willbold, M., Stracke, A., 2010. Formation of enriched mantle components by recycling of upper and lower continental crust. Chem. Geol. 276, 188–197.

Wood, B.J., Kiseeva, E.S., Matzen, A.K., 2013. Garnet in the Earth's mantle. Elements 9, 421–426.

Zhang, H.L., Cottrell, E., Solheid, P.A., Kelley, K.A., Hirschmann, M.M., 2018. Determination of $Fe^{3+}/\Sigma Fe$ of XANES basaltic glass standards by Mössbauer spectroscopy and its application to the oxidation state of iron in MORB. Chem. Geol. 479, 166–175.

Zimmer, M.M., Plank, T., Hauri, E.H., Yogodzinski, G.M., Stelling, P., Larsen, J., Singer, B., Jicha, B., Mandeville, C., Nye, C.J., 2010. The role of water in generating the calc-alkaline trend: new volatile data for Aleutian magmas and a new tholeiitic index. J. Petrol. 51, 2411–2444.